energies

MDPI

Article

Research on Noise Suppression Technology of Marine Optical Fiber Towed Streamer Seismic Data Based on ResUNet

Hongfei Qian, Xiangchun Wang *, Xuelei Chen and Zhu Yang

School of Geophysics and Information Technology, China University of Geosciences, Beijing 100083, China; 3010200014@cugb.edu.cn (H.Q.); xuelei0312@163.com (X.C.); 2110200049@cugb.edu.cn (Z.Y.)
* Correspondence: wangxc@cugb.edu.cn; Tel.: +86-137-1885-2383

Abstract: Optical fiber seismic exploration technology has been widely used in marine oil and gas hydrate exploration due to its wide frequency band and high sensitivity. However, there are more types of noise in the collected data by optical fiber hydrophone than by a conventional piezoelectric seismic exploration system. Considering that the conventional denoising method is time-consuming, this paper proposes a convolutional neural network (CNN) and a ResUNet network based on deep learning to suppress the noises. ResUNet is improved on the basis of CNN; it is composed of a feature extraction part, a feature reconstruction part and a residual block. Both CNN and ResUNet networks achieved obvious denoising effects on optical fiber towed streamer seismic data and improved the signal-to-noise ratio of data effectively. The ResUNet network has better denoising effects than CNN, even better than conventional denoising methods. The ResUNet network can solve the problem of gradient disappearance caused by network deepening; it recovered edge data well, and it has high efficiency compared with conventional denoising methods. Two evaluation indexes, relative error (RE) and similarity structure degree (SSIM), were introduced to compare the denoising effect of the ResUNet network with that of CNN. The experimental results showed that the performance of the ResUNet network in these two aspects is better than that of CNN.

Keywords: deep learning; ResUNet network; marine optical fiber towed streamer seismic; noise suppression; residual block; signal-to-noise ratio

Citation: Qian, H.; Wang, X.; Chen, X.; Yang, Z. Research on Noise Suppression Technology of Marine Optical Fiber Towed Streamer Seismic Data Based on ResUNet. *Energies* **2022**, *15*, 3362. https://doi.org/10.3390/en15093362

Academic Editor: Federico Barrero

Received: 7 April 2022
Accepted: 1 May 2022
Published: 5 May 2022

1. Introduction

In recent years, with the extensive development and utilization of energy and the promotion of the environmental protection concept, increasingly more people are focusing on the development of new energy resources in the ocean. As an important source of clean energy, natural gas hydrate has a high energy density and great resource potential [1]. In the process of natural gas hydrate exploration, seismic exploration is mainly used. The acquisition methods of marine seismic exploration include towed streamer seismic, ocean bottom seismometer (OBS), vertical cable seismic, etc.

Piezoelectric hydrophone and optical fiber hydrophone are commonly used in towed streamer data collection for marine seismic survey. Due to the low sensitivity and small dynamic range of piezoelectric hydrophones, optical fiber hydrophones have developed rapidly in the last 20 years and are increasingly used in marine seismic exploration. Optical fiber communication mainly modulates the signal into an optical signal for transmission through optical fiber. At the time of receiving the optical signal, the optical signal is demodulated to obtain the original information. Optical fiber hydrophone has good signal resolution, signal dynamic range and signal fidelity, and it can transmit seismic data quickly in large quantities. It also has the characteristics of wide band, high sensitivity and high frequency response, which greatly improve the quality of marine seismic data [2]. As early as 2000, the United States developed a 96-element optical fiber hydrophone system for natural gas exploration [3,4]. On this basis, Britain's QinetiQ placed hydrophones on the sea

floor and placed optical fiber cables and optical fiber accelerators on land [5]. In 2002, China carried out a sea test of an optical fiber hydrophone array with 23 elements in the Bohai Sea, which laid a good foundation for the development of optical fiber hydrophones [6]. In 2017, the Guangzhou Marine Geological Survey applied the optical fiber hydrophone array detection system to marine seismic exploration in the northern area of the South China Sea and obtained data by comparing the results with the piezoelectric hydrophone data; it was concluded that the optical fiber hydrophone can meet the performance requirements of marine seismic exploration.

However, a lot of noise is generated in marine seismic exploration when using optical fiber towed streamers, which will reduce the quality and signal-to-noise ratio of real seismic records and affect the accuracy of data processing and interpretation. In recent years, many researchers have applied CNN to seismic data denoising and found that CNN can improve the signal-to-noise ratio of seismic records.

A convolutional neural network was proposed by Yann LeCun of New York University in 1998 [7]. It was not until 2008 that CNN was applied to denoising for the first time. Jain et al. used CNN to obtain high-quality images from low-quality images [8]. In 2009, Viren Jain applied CNN to the process of natural image denoising and achieved good results. In 2012, Geoffrey et al. proposed a convolutional neural network called AlexNet, which made a great breakthrough in image recognition [9,10]. After the success of AlexNet, Visual Geometry Group (VGG) [11] at the University of Oxford, Google Net [12] with Google and other networks created better results consecutively. In 2015, He et al. proposed the Deep Residual Network (ResNet) [13] in ImageNet; the network has won the champion of image classification, detection and location. In the same year, Ronneberger et al. used the U-Net network in the microscope cell segmentation challenge [14]. Zhang et al. proposed a full convolutional denoising network based on residual learning in 2017, which uses a decomposition learning method combined with CNN to separate noise from noisy images [15]. With the increase in layers and trainable parameters of CNN, the trained network can well represent the nonlinear relationship between input and output, and combined with some traditional algorithms, CNN has achieved rapid development in many fields [16]. The ResUNet network used in this paper is based on CNN and a residual network, combined with an "encode-decode" structure to denoise seismic data. This network can solve the problem of gradient disappearance caused by the increase in network layers in CNN effectively, and the denoising effect is better than in the CNN. Compared with the identified works, the ResUNet proposed in this article used a convolutional operation, whose stride was increased, instead of a pooling operation, so as to avoid the loss of effective information, and achieved a very good effect.

2. Data Acquisition and Observation System

The data used in this study were collected by a ship named "Tan Bao Hao". The hardware collection system was developed by Beijing Appsoft Technology Co., Ltd., Beijing, China. The acquisition parameters were as follows. The source used in this acquisition was an air gun source: the shot points were 5 m below the sea surface, and the shot spacing was 25 m. The channel spacing was 3.125 m, and there was only one hydrophone per channel. The number of traces in one shot gather was 256, and the time sampling interval was 0.25 ms; the total record length was 7 s, so there were 28,000 sampling points per trace.

3. Noise Analysis of Marine Optical Fiber Data

In order to obtain high-quality seismic data from marine towed streamer seismic data acquisition, it is necessary to eliminate the influence of noise so as to obtain more useful information of target layers [1,17,18]. According to the characteristics, the interference waves in marine seismic exploration can be divided into two types, namely regular interference (coherent noise) and irregular interference (random noise) [19]. Regular interference has a strong regularity in its shape, such as linear interference. Irregular interference has no regularity in space and time, such as the noise caused by surge waves. Through the analysis

and study of various noises, we can understand the causes of its formation, which is helpful to eliminate or suppress them by using effective methods in the later data processing. For the practical data of marine optical fiber to be processed this time, its noise analysis is as follows.

Figures 1a, 1b and 1c are single-shot records of different seawater depths, respectively, of which Figure 1a is the shallowest, and Figure 1c is the deepest. It can be found that the types and characteristics of noise at different sea depths are different.

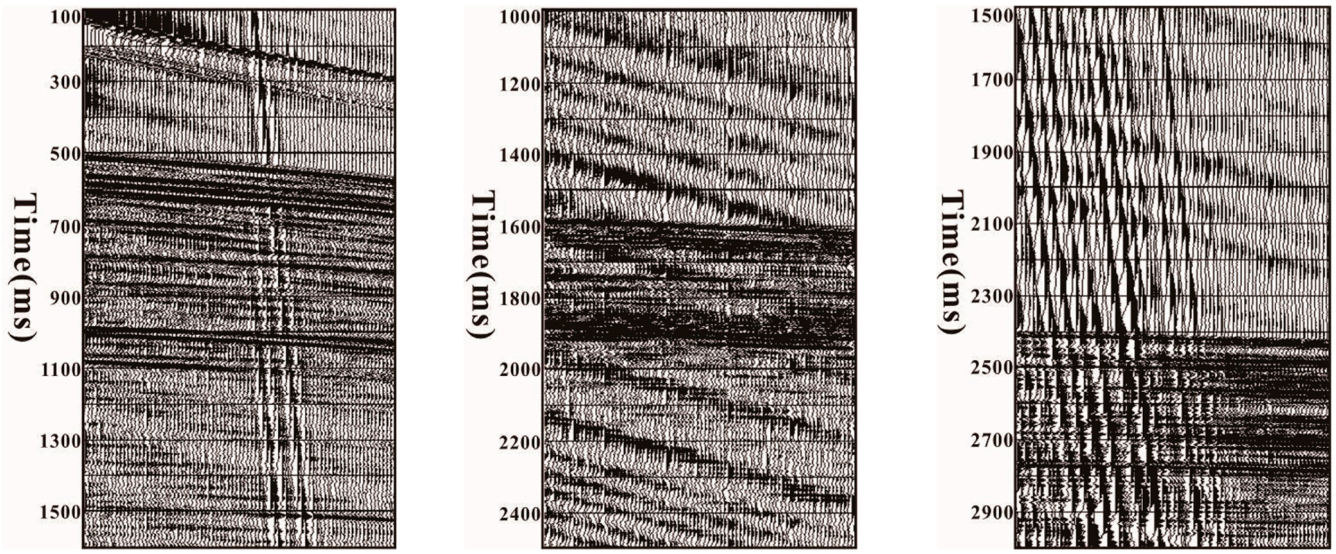

(**a**) (**b**) (**c**)

Figure 1. Single shot records of three different seawater depths. (**a**) is the shallowest; (**b**) is intermediate depth; (**c**) is the deepest.

As shown in Figure 2, it can be observed that periodic noise occurs in space every 16 traces, which is characterized by regular and equal spacing. A long optical fiber streamer is composed of multiple short streamers, so it is speculated that regular noise was generated by the connection of the short streamers.

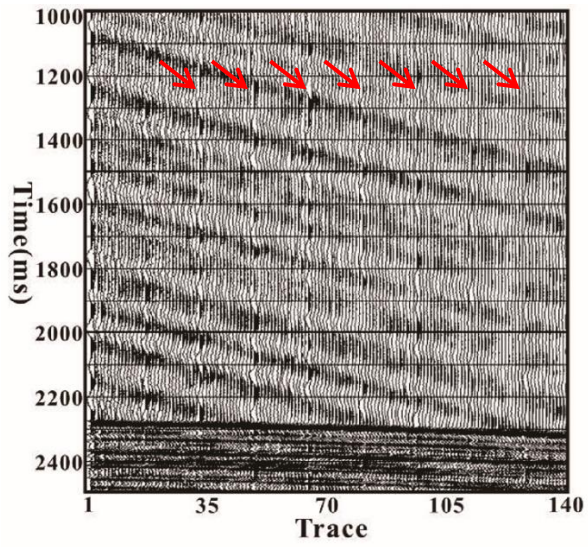

Figure 2. Spatial periodic noise. The red clippers indicate the spatial noise occurring every 16 traces.

Another common noise in marine seismic exploration is surge wave noise, which has low frequency, strong energy, and randomness. In conventional surge noise, the dominant

frequency of the surge is 3 Hz. As shown in Figure 3, the frequency spectrum analysis of surge wave noise shows that the dominant frequency is around 4 Hz, with a speed of about 34 m/s.

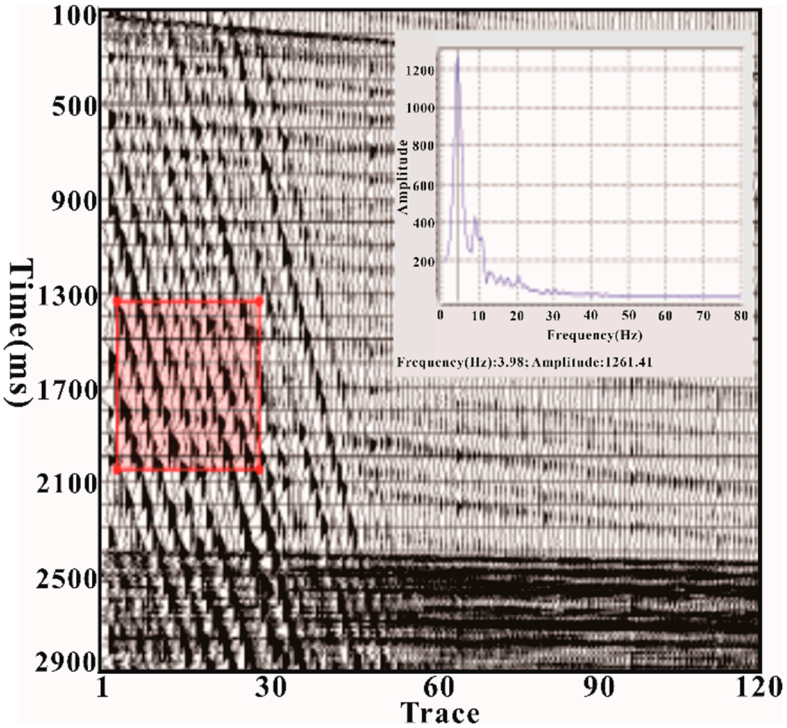

Figure 3. Surge noise.

After further analysis of the data, it was found that linear noise appeared from the shooting end to the receiving end and from the receiving end to the shooting end, as shown in Figure 4a,b. The two kinds of linear noises have the same morphology and similar velocities, about 1080 m/s, only opposite in direction. Therefore, it is speculated that these two linear noises were caused by the vibration of the ship and the vibration of the tail buoy, respectively. The ship vibrated while moving, and the buoys on the stern vibrated together. These vibrations were quite regular. The vibration of the ship caused linear noise from the shooting end to the receiving end, and in contrast, the vibration of the buoy caused linear noise from the receiving end to the shooting end.

To sum up, there are three kinds of noise for marine optical fiber towed streamer seismic data: surge wave noise, linear noise from ship vibration and periodic noise from instrument connections. In addition, the noise of each shot is different, so in the process of processing the optical fiber streamer data, the noise removal is the most difficult step but is important. Conventional seismic data processing needs to remove each kind of noise separately, which is complex. Therefore, it is proposed to use artificial intelligence technology to build ResUNet for marine optical fiber towed streamer seismic data denoising, which has high efficiency.

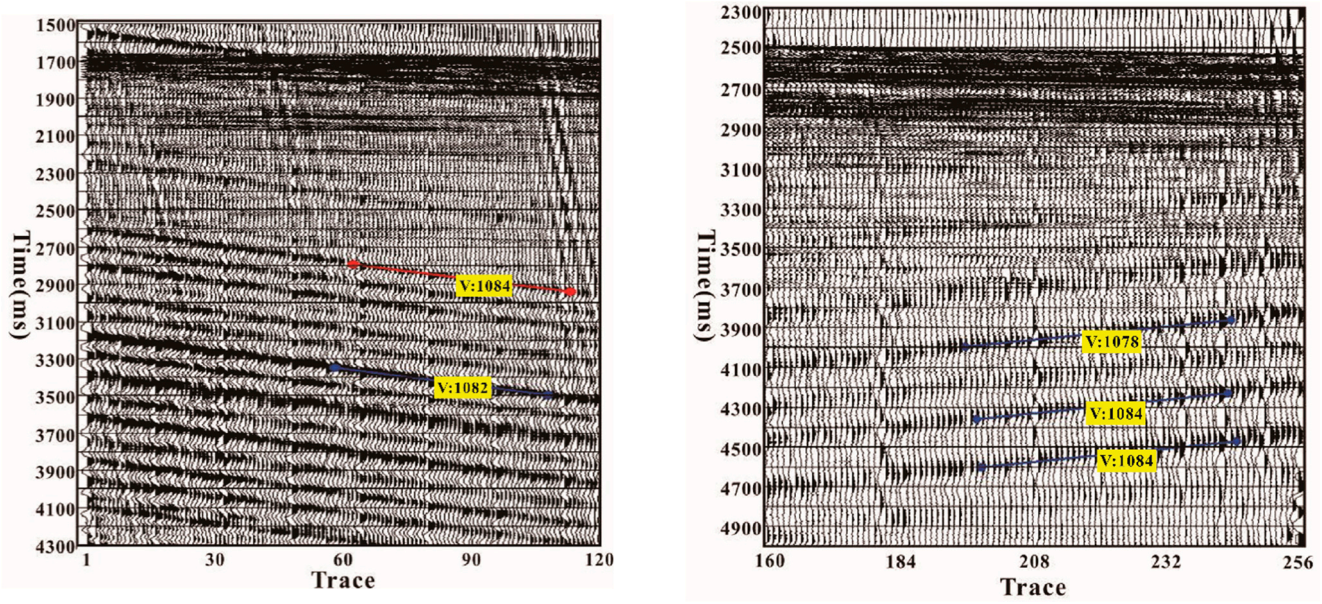

(**a**) (**b**)

Figure 4. Linear noise generated by ship vibration and tail buoy vibration. (**a**) is the linear noise generated by ship vibration; (**b**) is the linear noise generated by tail buoy vibration.

4. ResUNet Network

4.1. ResUNet Principle

The ResUNet network improves upon CNN; it combines the residual block and adds an "encoding-decoding" structure. The "encoding-decoding" structure is also called U-NET, because its structure resembles the letter "U". The ResUNet structure combines the advantages of a residual network and a U-NET network. ResUNet is established on the basis of a U-NET network, and a residual unit is added as the basic unit to replace ordinary neurons [20].

The U-NET network consists of two parts. The first part is an encoding part, also called down-sampling: in this part, the convolution operation is used to extract the data features and using the pooling operation to reduce the size of the data. When the data size is larger, a convolution kernel obtains information of the data; as the data size gradually decreases, the convolution kernel gradually acquires the outline information of the data. Then, the whole network obtains all the information of the large-sized data and the small-sized data. In the second part of the network, an up-sampling operation is used to expand and restore the data to the size of the original data [21]. Meanwhile, combined with skip connection operation, it is used to integrate the information from data of the same size in the down-sampling, and the up-sampling retains the structural information of each level so that the entire network can remember all the information of the data. However, when the network is too deep, the gradient will disappear in the back propagation. Therefore, ResNet is proposed and combined with U-Net to solve this problem.

The idea of a ResNet network mainly lies in identity mapping [22]. Identity mapping is added to the network; that is, the input is added to the output layer. Experiments had found that this operation will not increase the error of a training set when the network depth is increasing [23]. However, it is difficult to learn identity mapping directly in deep network, so He et al. proposed the idea of residual learning. Figure 5 is a schematic diagram of a residual block. Assuming that x is the input and $H(x)$ is the identity mapping that requires to solved, $F(x) = H(x) - x$ is the residual, solving the residual function $F(x)$ as the objective. Then, the input x is directly added to the output layer, so the $H(x)$ can be expressed as $H(x) = F(x) + x$. In this case, $H(x)$ is obtained by summing the two components; the benefit of doing this is that when the network has reached the optimum, continuing to deepen

the network, $F(x)$ will be set to zero, so $H(x) = x$, which means the network will always remain optimal, and the performance of the network will not degrade as the number of layers increases. Meanwhile, in the process of back propagation, the gradient is transmitted between the two residual blocks, and the gradient before the derivation is added, which is equivalent to increasing the gradient artificially and reducing the possibility of gradient disappearance [24].

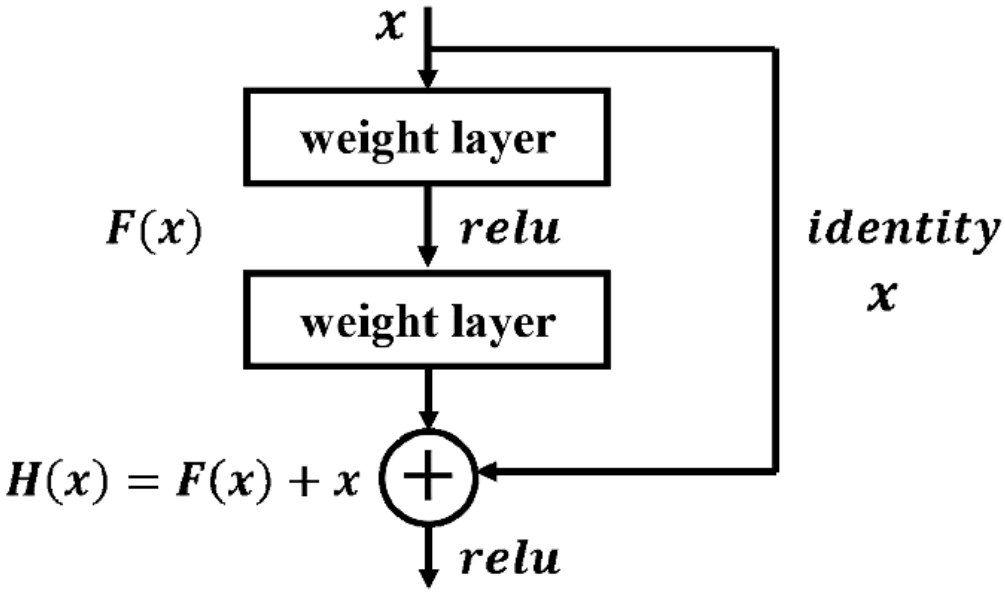

Figure 5. Basic structure of residual block.

U-net realizes the network's recognition of multi-scale features, and in the process of up-sampling, its output integrates the output of down-sampling; in fact, the multi-scale features are fused together. In order to solve the problem of gradient disappearing, a ResUNet network is proposed by combining ResNet with U-NET [25].

4.2. Structure of ResUNet

Based on the analysis of noise in the data and the characteristics of ResUNet, the structure of the ResUNet network constructed in this paper is shown in Figure 6.

It should be noted that the network constructed in this paper does not use a pooling operation when encoding to shrink the data size, but we added a convolutional layer between two residual units and set its stride to 2 in order to reduce the data size. In the process of pooling operation to reduce the dimension, this will cause the loss of effective signals of seismic data and high computational complexity, thus increasing the stride in the convolutional layer instead of the pooling operation.

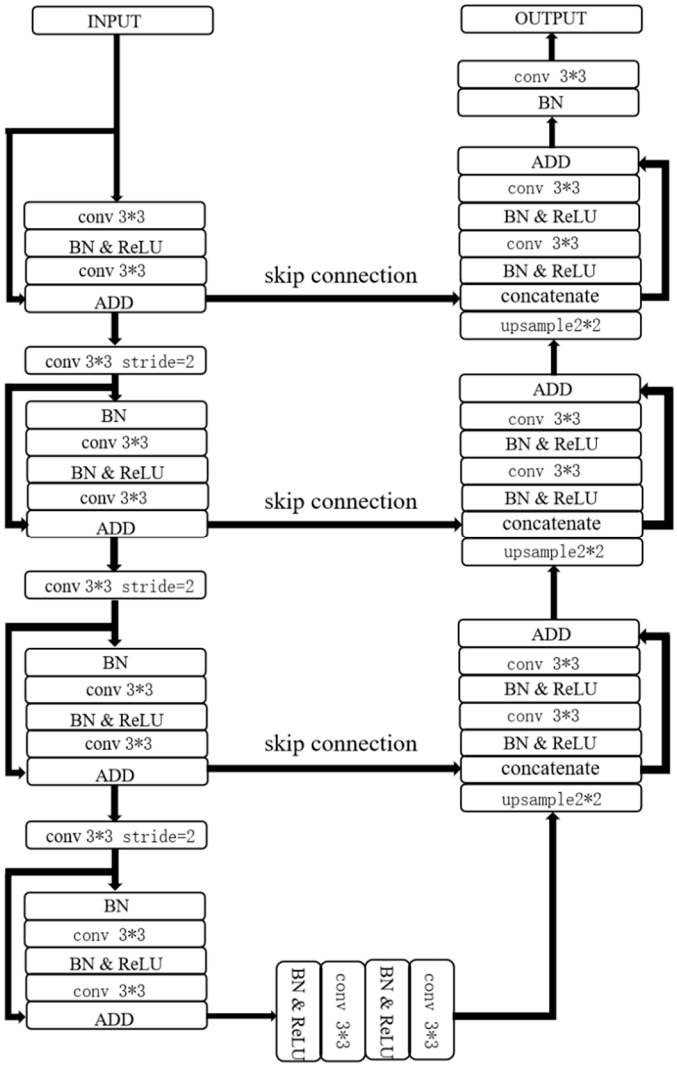

Figure 6. ResUNet network structure constructed in this paper.

5. ResUNet Denoised the Practical Optical Fiber Towed Streamer Data

5.1. Data Preparation and Denoising

First of all, the original data were processed to remove the bad trace. Then, using the Geoeast3.0 software to remove the surge noise, the coherent noise was suppressed, the abnormal amplitude was removed, and the spatial periodic noise was filtered. The Geoeast3.0 was created by Bureau of Geophysical Prospecting INC, China National Petroleum Corporation, Hebei, China. The original single-shot recording had 256 traces and 28,000 sampling points per trace. In order to reduce the training pressure, it was resampled to 3500 sampling points per trace, and 1600 sampling points were selected in the middle. Because there were too many shots in a set of data, when using conventional methods to denoise, all the shots were processed simultaneously, which caused the denoising effect of each shot to be uneven. Based on this, when selecting label data, 50 shots with good denoising effect were selected as training samples. The original data and label data are shown in Figures 7 and 8.

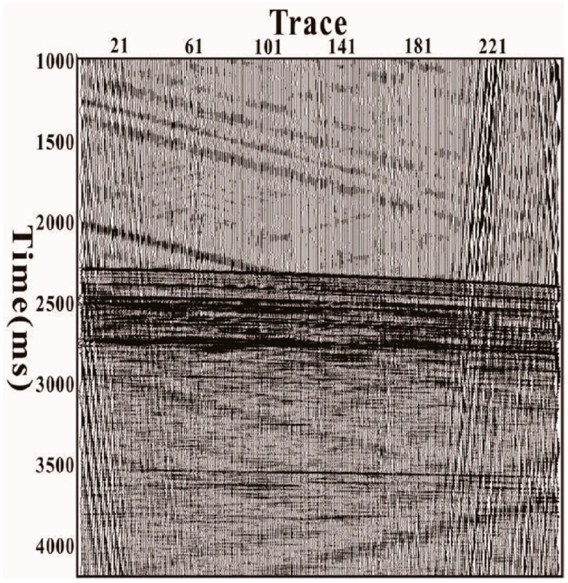

Figure 7. Original single shot data.

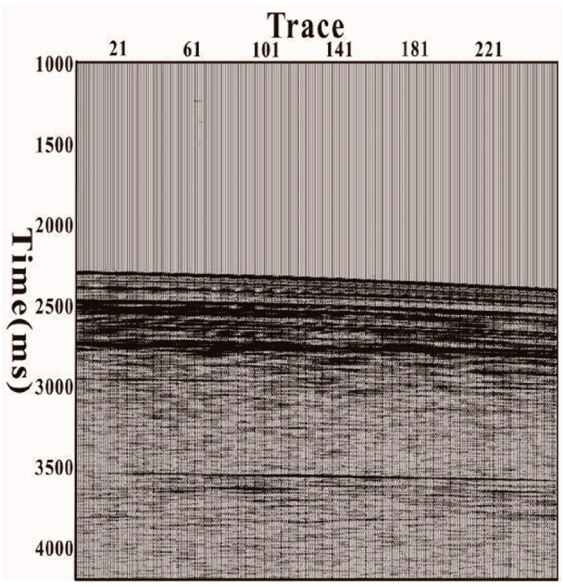

Figure 8. Single shot label data.

In order to compare with ResUNet network, this paper also constructed a CNN, whose structure is shown in Figure 9, using the same data and using two networks for training, respectively.

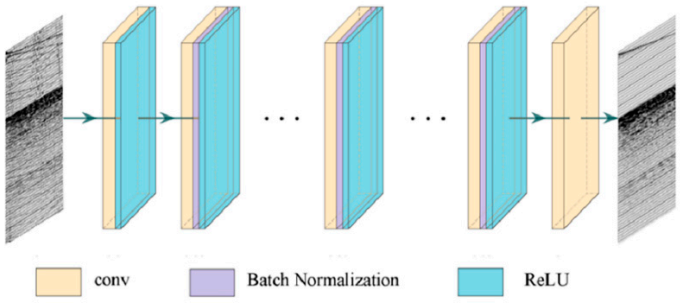

Figure 9. Structure of convolutional neural network.

Conv refers to the convolution layer, and the convolution kernel is used to extract the features of the input data. The purpose of the batch normalization is to make the data output from each convolutional layer have the same distribution, thus ensuring the gradient descent process is more stable. ReLU is the activation function, which can solve the nonlinear problems to enhance the complexity of the network.

The training epochs are set to 20. The error decline curves of the two networks are shown in Figures 10 and 11. The ordinate represents the mean square error (*MSE*), and the abscissa represents the training times. The *MSE* is defined as follows:

$$MSE = \frac{1}{n}\sum_{i=1}^{n}\left|y_i - y_i'\right|^2 \quad (1)$$

where y represents the data before training, and y' represents the data after training.

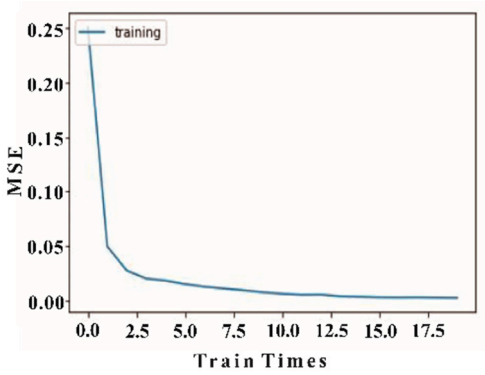

Figure 10. ResUNet error decline curve.

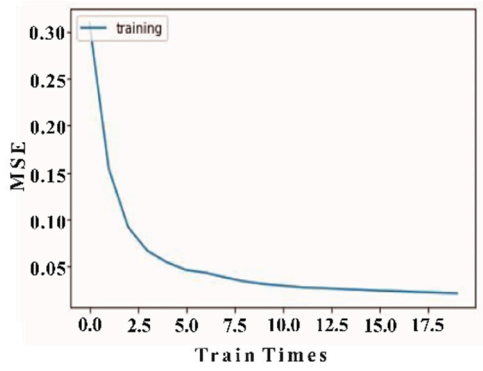

Figure 11. CNN error decline curve.

It can be found that the *MSE* of ResUNet is lower than that of CNN after convergence.

5.2. Visual Analysis

Visualize the training process of output layer in ResUNet. Figure 12a, Figure 12b and Figure 12c are the output results of the output layer after the first, 10th and 20th training epoch, respectively. With the increase in training epochs, the oblique noise below the efficient signal is obviously suppressed, the performance of details is more and more obvious, and the output image comes closer to the target image. The results of Figure 12b,c are relatively close, because in the first few epochs of training, the error curve converges faster, while the latter half converges slower and slower.

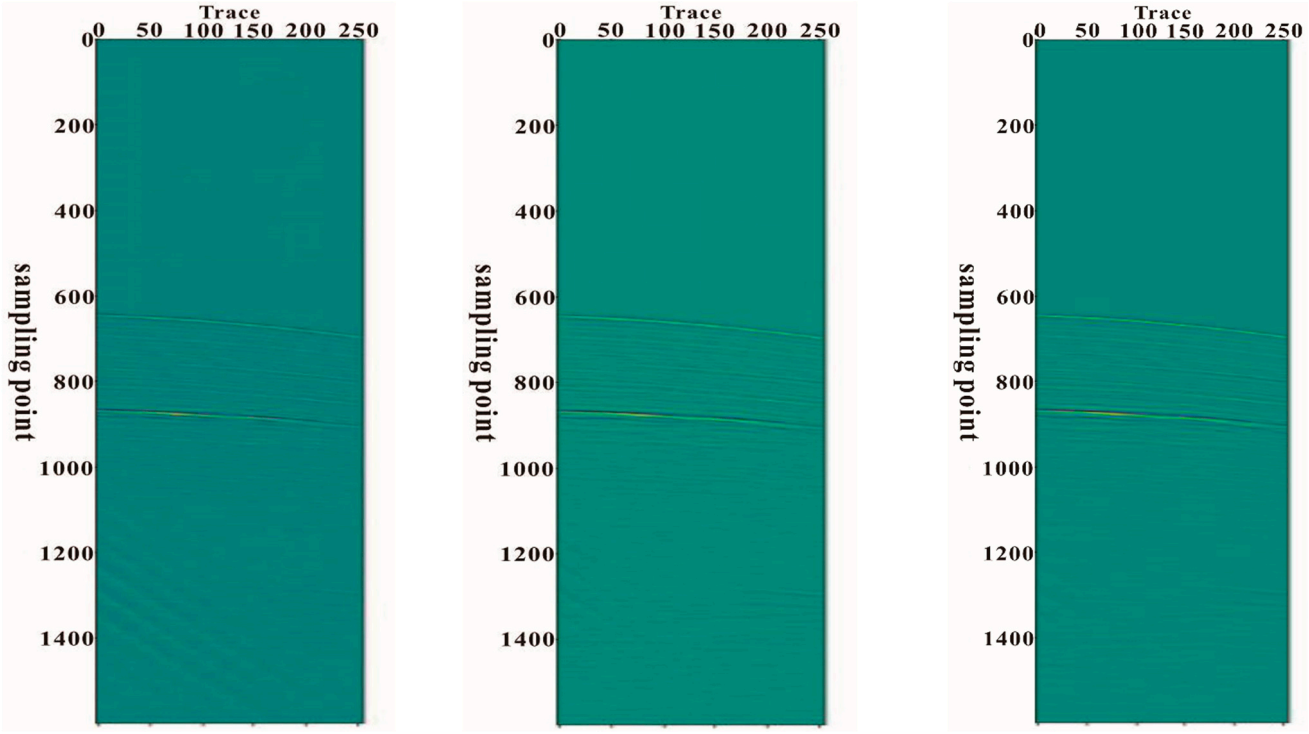

Figure 12. Output results of the output layer after different training epochs. (**a**) is the 1st training; (**b**) is the 10th training; (**c**) is the 20th training.

Figure 13a–f are the output of some intermediate layers in the last training epoch. In the process of down-sampling, the input data with a size of 256 × 1600 are compressed into 32 × 200 abstract features to obtain data of different scales, and the resolution of the image continuously reduces. Meanwhile, the number of feature maps gradually increases. The process of up-sampling is mainly used to recover target details; the feature maps extracted from the down-sampling are combined with the reconstructed information from the up-sampling by skip connection to shorten the time of network training [26]. Then, this is compared with the label data in the output layer, the error is calculated, and back propagation is performed.

5.3. Results Analysis

After the network training was completed, we selected the single shot records whose denoising effect was not ideal by conventional denoising methods. CNN and ResUNet were used for denoising, respectively. The original data and denoising results are as follows.

As shown in Figure 14, Figure 14a is the original single shot data to be denoised. Serious oblique interference is developed in the data, and there is also obvious interference in the longitudinal direction. Figure 14b is the denoising results of the commercial software Geoeast, and Figure 14c is the denoising result of the CNN. It can be found that Geoeast software and CNN have an obvious effect on noise removal, and the useful information is effectively restored, but the shortcoming of both is that the linear noise above the reflection signal is not completely removed. From the denoising results of CNN, it can be found that the signal recovery is not sufficient at either end of the reflection wave, and some edge information is lost. Figure 14d shows the denoising effect of the ResUNet network constructed in this paper. From the denoising results of ResUNet, we see that the edge information is well-recovered without loss, and the linear noise removal effect above the reflection wave is significantly better than that of CNN, and even better than that of Geoeast.

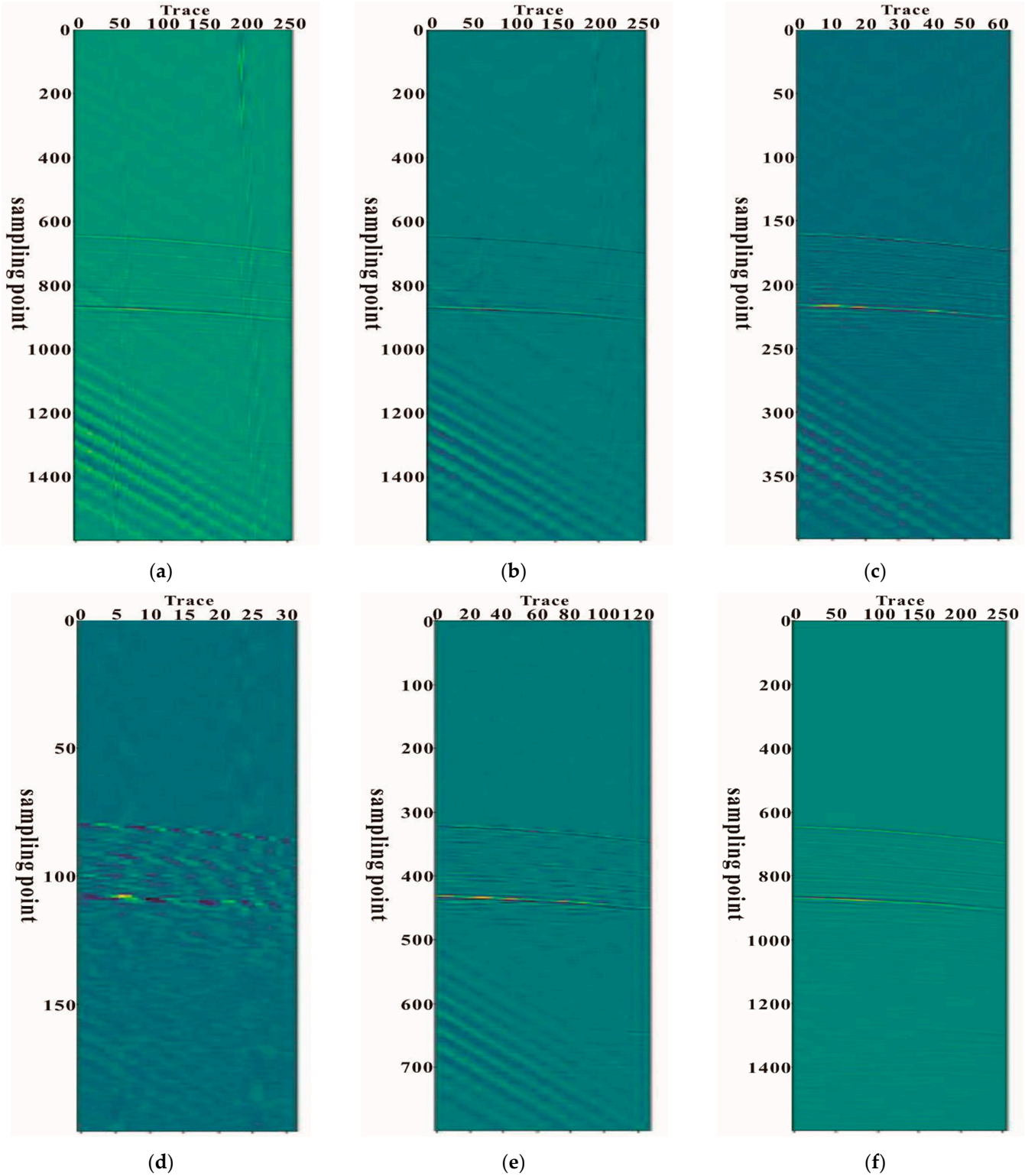

Figure 13. Output results of the last epoch of some middle layers. (**a**) is the 1st layer; (**b**) is the 6th layer; (**c**) is the 20th layer; (**d**) is the 27th layer; (**e**) is the 42nd layer; (**f**) is the 60th layer.

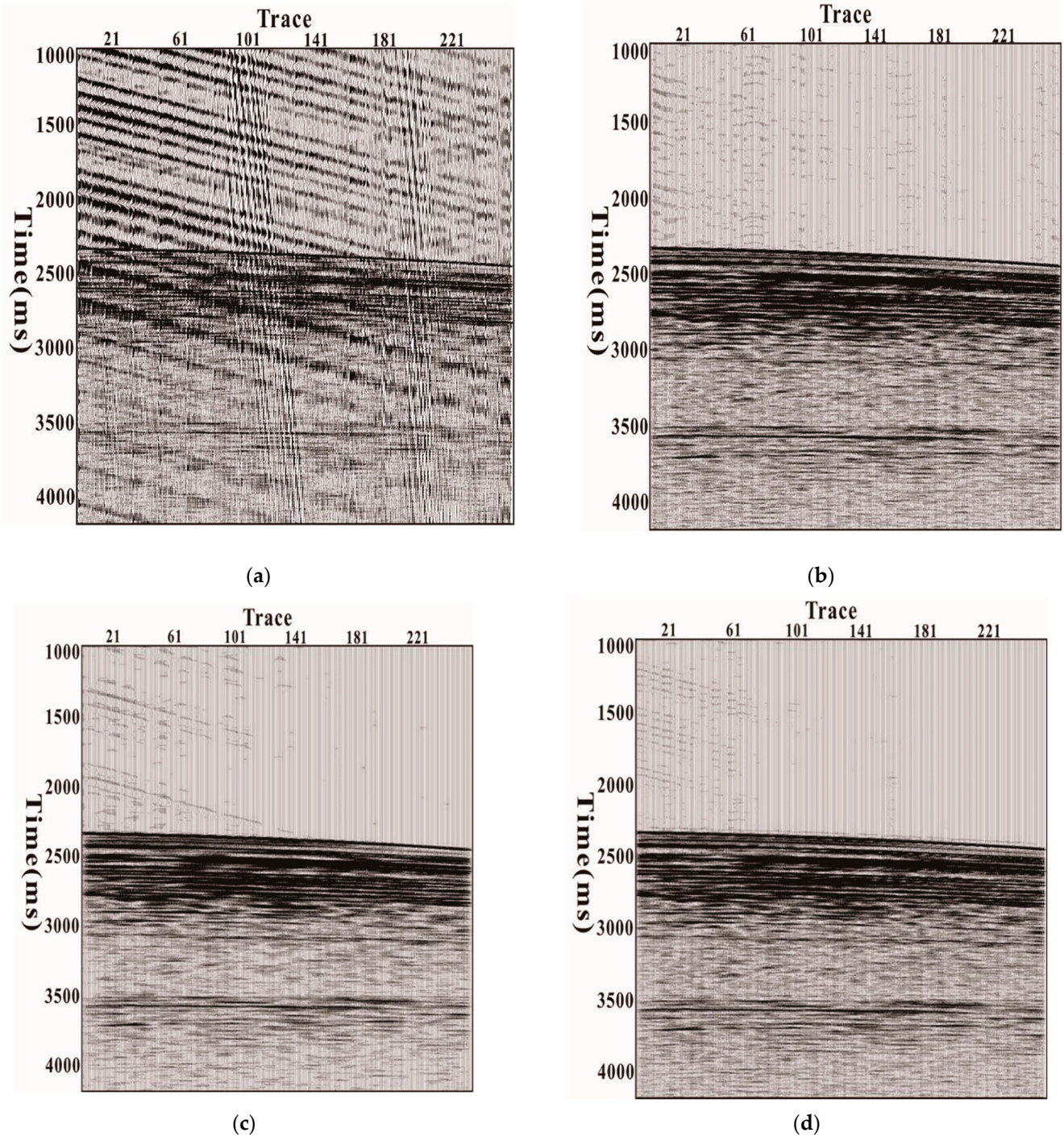

Figure 14. (**a**) is original data; (**b**) is the denoising result of software Geoeast; (**c**) is the denoising result of CNN; (**d**) is the denoising result of ResUNet.

5.4. Evaluation Index

In order to evaluate the denoising effect of the two networks, relative error (*RE*) [26] and structural similarity (*SSIM*) [27] are introduced. The relative error is defined as follows:

$$RE = \frac{\| A - A' \|}{\| A' \|} \tag{2}$$

Among them, A represents the original seismic data, A' represents the denoised seismic data, and $\| x \|$ represents the norm:

$$\| x \| = \sqrt{\sum_{m=1}^{n} x_m^2} \tag{3}$$

The definition of structural similarity is as follows:

$$SSIM = \frac{(2\mu_A\mu_{A'} + C_1)(2\sigma_{AA'} + C_2)}{(\mu_A^2 + \mu_{A'}^2 + C_1)(\sigma_A^2 + \sigma_{A'}^2 + C_2)} \tag{4}$$

where A and A', respectively, represent the original seismic data and the denoised seismic data, μ_A and $\mu_{A'}$, respectively, represent the average value of A and A'. σ_A^2 and $\sigma_{A'}^2$, respectively, represent the variance of A and A'. $\sigma_{AA'}$ is the covariance of A and A'. In addition, $C_1 = (k_1 L)^2$ and $C_2 = (k_2 L)^2$ are constants used to ensure the stability of the equation, where L represents the dynamic range of data, L is usually 255, k_1 is usually 0.01, and k_2 is usually 0.03 [28].

As shown in Table 1, the smaller the *RE* and *MSE* value is, the better the denoising effect is, while the closer the value of *SSIM* is to 1, the more similar the structure of denoised data is to the original data. It can be found that, compared with the traditional CNN, the denoised result of ResUNet shows better performance in the analysis of *RE*, *SSIM* and *MSE*.

Table 1. *RE*, *SSIM* and *MSE* values of denoising effects of different network types.

Evaluation Index / Network Type	*RE*	*SSIM*	*MSE*
CNN	0.2925	0.92	0.0204
ResUNet	0.1604	0.96	0.0074

6. Discussion and Conclusions

Aiming at the problem of noise suppression in marine optical fiber towed streamer seismic data, this paper proposed a data denoising method based on deep learning. We constructed a network named ResUNet, which consisted of ResNet and U-Net. The data with good denoising effect of the conventional algorithm were selected as the training set to train the ResUNet network, and then we selected the data with unsatisfactory denoising effect of conventional algorithms to input the network for denoising. It can be found that, compared with the traditional denoising method, this method has a higher efficiency, and ResUNet also has good denoising performance when the denoising effect of traditional methods is not ideal.

In order to verify the denoising effect of ResUNet, this paper also built a CNN for comparison. The denoising results show that ResUNet is significantly better than CNN in the recovery of edge effective signals. Two evaluation indicators of RE and SSIM showed that the denoising ability of ResUNet is stronger than that of the CNN. Therefore, the ResUNet proposed in this article can be applied to other seismic data denoising; as long as the label data have a good effect, the final denoising effect is also satisfactory. In future research, the generalization of network is worth studying, and how to train the network when conventional denoising methods are not ideal is also an interesting issue.

Author Contributions: Conceptualization, X.W.; methodology, H.Q.; software, X.W. and H.Q.; resources, X.W.; writing—original draft preparation, H.Q.; writing—review and editing, X.W.; visualization, X.C.; supervision, Z.Y.; project administration, X.W. All authors have read and agreed to the published version of the manuscript.

Funding: This research was funded by the National Natural Science Foundation of China, grant number 41874131.

Institutional Review Board Statement: Not applicable.

Data Availability Statement: Not applicable.

Conflicts of Interest: The authors declare no conflict of interest.

References

1. Zhang, G.; Xu, H.; Liu, X.; Zhang, M.; Wu, Z.; Liang, J.; Wang, H.; Sha, Z. The acoustic velocity characteristics of sediment with gas hydrate revealed by integrated exploration of 3D seismic and OBS data in Shenhu area. *Chin. J. Geophys.* **2014**, *57*, 1169–1176.
2. Wang, X.; Li, X.; Zhang, H.; Hao, X.; Yu, K. Optical fiber marine seismic exploration system feasibility study. *Acta Geophys.* **2019**, *67*, 1403–1411. [CrossRef]
3. Zhang, R.; Ni, M. Principle and applications of the fiber optic hydrophone. *Physics* **2004**, *33*, 503–507.
4. Hong, X.; Lang, S.; Zheng, L. Characteristics of Fiber Hydrophones and its Research Situation. *J. Chang. Inst. Technol.* **2006**, *06*, 36–40.
5. Chen, Z. Research on High-Speed Data Acquisition and Real-time Processing of Fiber Optic Hydrophone System. Master's Thesis, Central South University of Forestry and Technology, Changsha, China, 2009.
6. Hao, X.; Zhang, H.; Wei, C.; Wang, C.; Zhang, H. Sea trial for fiber-optic hydrophone array used in marine geophysical exploration. *J. Trop. Oceanogr.* **2018**, *37*, 93–98.
7. Gu, H. Denoising of Seismic Data Based on Convolution Neural Network. Master's Thesis, Northeast Petroleum University, Daqing, China, 2019.
8. Jain, V.; Seung, H.S. Natural image denoising with convolutional networks. In Proceedings of the International Conference on Neural Information Processing Systems, Auckland, New Zealand, 25–28 November 2008.
9. Xue, D. Research on Cancer Image Recognition Based on Convolutional Neural Networks. Ph.D. Thesis, University of Science and Technology of China, Hefei, China, 2017.
10. Krizhevsky, A.; Sutskever, I.; Hinton, G.E. ImageNet classification with deep convolutional neural networks. *Commun. ACM* **2017**, *60*, 84–90. [CrossRef]
11. Zhen, X.; Chen, J.; Zhong, Z.; Hrycushko, B.; Zhou, L.; Jiang, S.; Albuquerque, K.; Gu, X. Deep convolutional neural network with transfer learning for rectum toxicity prediction in cervical cancer radiotherapy: A feasibility study. *Phys. Med. Biol.* **2017**, *62*, 8246–8263. [CrossRef]
12. Szegedy, C.; Liu, W.; Jia, Y.; Sermanet, P.; Reed, S.; Anguelov, D.; Erhan, D.; Vanhoucke, V.; Rabinovich, A. Going deeper with convolutions. In Proceedings of the IEEE Computer Society Conference on Computer Vision and Pattern Recognition, Boston, MA, USA, 7–12 June 2015; pp. 1–9.
13. He, K.; Zhang, X.; Ren, S.; Sun, J. Deep Residual Learning for Image Recognition. In Proceedings of the IEEE Conference on Computer Vision and Pattern Recognition (CVPR), Las Vegas, NV, USA, 27–30 June 2016.
14. Ronneberger, O.; Fischer, P.; Brox, Y. Convolutional networks for biomedical image segmentation. *Med. Image Comput. Comput.-Assist. Interv.* **2015**, *9351*, 234–241.
15. Zhang, K.; Zuo, W.; Chen, Y.; Meng, D.; Zhang, L. Beyond a Gaussian Denoiser: Residual Learning of Deep CNN for Image Denoising. *IEEE Trans. Image Process.* **2017**, *26*, 3142–3155. [CrossRef]
16. Wang, J. Recognition of License Plate Character by Deep Learning. *Ind. Control Comput.* **2017**, *30*, 51–52.
17. Chen, J.; Zhuang, X.; Hu, B.; Zhang, J.; Wang, Z. Application of the Combination Method to Multiple Attenuation in Marine Seismic Data Processing. *Mar. Orig. Pet. Geol.* **2011**, *1*, 68–73.
18. Wang, H.; Ding, Z.; Gui, D.; Huang, J. Application of seismic source wavelet deconvolution in marine seismic survey. *Geophys. Prospect. Pet.* **2013**, *52*, 49–54.
19. Zhang, W.; Yang, Z.; Chen, C. Formation and Identification of Offshore Original Seismic Data Interference Wave. *China Pet. Explor.* **2011**, *4*, 65–69.
20. Zhang, Z.; Liu, Q.; Wang, Y. Road Extraction by Deep Residual U-Net. *IEEE Geosci. Remote Sens. Lett.* **2018**, *15*, 749–753. [CrossRef]
21. Wang, Y.; Lu, W.; Liu, J.; Zhang, M.; Miao, Y. Random seismic noise attenuation based on data augmentation and CNN. *Chin. J. Geophys. Chin. Ed.* **2019**, *62*, 421–433.
22. Zeng, Z.; Xie, W.; Zhang, Y.; Lu, Y. RIC-Unet: An Improved Neural Network Based on Unet for Nuclei Segmentation in Histology Images. *IEEE Access* **2019**, *7*, 21420–21428. [CrossRef]
23. Wei, X.; Xing, J.; Wang, Z.; Wang, Y.; Shi, J.; Zhao, D.; Wang, H. Magnetic resonance image segmentation of articular synovium based on improved U-Net. *J. Comput. Appl.* **2020**, *40*, 3340–3345.
24. Gong, Y.; Huang, M.; Huang, X. Research on flame image segmentation method based on improved ResNet-UNet. *J. Beijing Inf. Sci. Technol. Univ.* **2021**, *36*, 39–44.
25. Luo, R.; Li, Y. Random seismic noise attenuation based on RUnet convolutional neural network. *Geophys. Prospect. Pet.* **2020**, *59*, 51–59.
26. Fu, R.; Zhang, X.; Wang, Z.; Wang, D.; Chen, X. Electrical impedance tomography method based on V-ResNet. *Chin. J. Sci. Instrum.* **2021**, *42*, 279–287.

27. Zhu, X.; Yao, S.; Sun, B.; Qian, Y. Image quality assessment: Combining the characteristics of HVS and structural similarity index. *J. Harbin Inst. Technol.* **2018**, *50*, 121–128.
28. Zheng, Y. Attenuation of Coherent Noise Based on Convolutional Neural Network. Master's Thesis, China University of Geosciences, Beijing, China, 2020.